Pattern Formation and Exotic Order in Driven-Dissipative Bose-Hubbard Systems

Zijian Wang,[1,2] Carlos Navarrete-Benlloch,[1,3] and Zi Cai[1,3,4,*]

[1]Wilczek Quantum Center, School of Physics and Astronomy, Shanghai Jiao Tong University, Shanghai 200240, China
[2]Zhiyuan College, Shanghai Jiao Tong University, Shanghai 200240, China
[3]Shanghai Research Center for Quantum Sciences, Shanghai 201315, China
[4]Key Laboratory of Artificial Structures and Quantum Control, Department of Physics and Astronomy, Shanghai Jiao Tong University, Shanghai 200240, China

(Received 18 February 2020; accepted 17 August 2020; published 9 September 2020)

Modern experimental platforms such as superconducting circuit arrays call for the exploration of bosonic tight-binding models in unconventional situations with no counterpart in real materials. Here we investigate one such situation in which excitations are driven and damped by pairs, leading to pattern formation and exotic bosonic states emerging from a nonequilibrium quantum many-body system. Focusing on a two-dimensional driven-dissipative Bose-Hubbard model, we find that its steady states are characterized by the condensation of bosons around momenta lying on a "Bose surface," a bosonic analog of the Fermi surface in solid-state systems. The interplay between instabilities generated by the driving, the nonlinear dissipative mode coupling, and the underlying lattice effect allows the system to equilibrate into an exotic superfluid state of bosons condensed on a closed ring in momentum space instead of discrete points. Such an unconventional state with a spatially uniform density distribution goes beyond the traditional scope of pattern formation and thus has no counterpart in the classical literature. In addition, it is a state connected to several open problems in modern condensed-matter physics. Here we provide the means to stabilize it, opening the way to its experimental study. Moreover, we also provide a concrete experimental implementation of our model in currently available superconducting circuit arrays. We also investigate the relaxation spectrum around the condensate, which shows a characteristic purely diffusive behavior.

DOI: 10.1103/PhysRevLett.125.115301

Introduction.—The scope of nonequilibrium physics is immense since the universe as a whole is a nonequilibrium system. A fundamental question in this context is understanding how the observed richness of spatiotemporal patterns spontaneously emerges from nothing [1]. In contrast to pattern formation within thermodynamic equilibrium, rooted in the minimization of (free) energy, patterns emerging in nonequilibrium systems can only be understood within a dynamical framework, even if the patterns of interest are time independent. More often than not, when a system is driven far from equilibrium, spatially uniform structures become unstable toward the growth of small perturbations, which leads to dynamics that amplify fluctuations and increase complexity. Late-time dynamics is dominated by the fastest-growing fluctuating modes, whose characteristic length and timescales determine the resulting spatiotemporal patterns, eventually stabilized by nonlinear and dissipative mechanisms [2]. In such a dynamical framework, dynamical instabilities and nonlinear mode coupling mechanisms are crucial for pattern formation [3].

Nonequilibrium pattern formation has been intensively studied in classical systems ranging from hydrodynamics [4] and cosmology [5] to biochemistry [6] and optics [7–10]. A profound question, then, is how to generalize these ideas to nonequilibrium quantum systems where the interplay between the intrinsic quantum fluctuations and external nonequilibrium conditions might give rise to richer phenomena than what is expected on the basis of these effects separately [11–13]. The situation is further complicated and potentially richer when the quantum system is an interacting many-body system, opening avenues for observing exotic quantum states of matter that are absent in either equilibrium quantum systems or in nonequilibrium classical systems. Recently, significant experimental progress has been made in Bose-Einstein condensates (BECs), where stripes, squares, hexagons, and other types of patterns have been observed in exciton-polaritons [14,15] and ultracold atoms [16–24]. But besides these conventional patterns, it is even more interesting to investigate exotic nonequilibrium states inspired by the intrinsic quantum nature of these systems that have not been discussed in their classical counterparts.

In this Letter, we study pattern formation and exotic order in the nonequilibrium steady states of a pair-driven-dissipative Bose-Hubbard (BH) model, for which we propose a concrete implementation based on current superconducting circuit arrays. In contrast to the continuous systems studied previously [14,15], here we investigate a tight-binding model defined on a two-dimensional (2D)

square lattice, where many-body effects are known to play a crucial role in determining equilibrium phase diagrams [25]. To drive the system out of equilibrium, we consider local pair creation and annihilation terms (pair driving) that induce spatially dependent instabilities determined by the fastest growing modes, which, as we show, lie on the Bosonic analog of a Fermi surface. We include the nonlinear dissipation that unavoidably accompanies pair driving and serves to stabilize the system. We consider two distinct situations. First, we consider a situation in which the Bose surface is a generic closed curve, leading to unconventional superfluid states forming striped density patterns. Then, we consider a so-called nested surface for which we obtained an exotic state with bosons condensed on a closed ring instead of discrete points in the Brillouin zone, leading to a spatially uniform density but with a nontrivial phase distribution. In equilibrium physics, similar Bose-liquid states have been conjectured to play an important role in frustrated quantum magnetism [26], high-T_c superconductors [27], and cold atoms with spin-orbit coupling [28,29]. We also discuss the relaxation spectrum of fluctuations around the generic condensate, showing that it is dominated by a purely diffusive mode.

Model and method.—We study a 2D BH model in a square lattice with on-site pair creation or annihilation, governed by the Hamiltonian

$$\frac{\hat{H}}{\hbar} = -J\sum_{\langle ij\rangle}\hat{b}_i^\dagger\hat{b}_j + \frac{1}{2}\sum_i\left(\frac{U}{2}\hat{b}_i^{\dagger 2}\hat{b}_i^2 - \nu\hat{n}_i + \frac{\Delta}{2}\hat{b}_i^2\right) + \text{H.c.}, \tag{1}$$

where $\hat{b}_i$ annihilates a boson at site $\boldsymbol{i}$ and $\hat{n}_i = \hat{b}_i^\dagger\hat{b}_i$ is the corresponding number operator. J is the single-particle hopping rate between adjacent lattice sites $\langle\boldsymbol{ij}\rangle$. ν resembles the chemical potential of equilibrium systems, but in our nonequilibrium setup it can be tuned from positive to negative [30]. Δ is the pair-driving rate, which we take as positive without loss of generality. In a conventional BH model, U is the interaction rate, but in our dissipative model it will adopt a more general meaning that we discuss later.

To get a better understanding of the effect of pair driving, we focus first on the $U = 0$ case. The Hamiltonian takes a quadratic form with translational invariance, which is written in momentum space as

$$\frac{\hat{H}}{\hbar} = \sum_{\boldsymbol{k}}(\varepsilon_{\boldsymbol{k}} - \nu)\hat{b}_{\boldsymbol{k}}^\dagger\hat{b}_{\boldsymbol{k}} + \frac{\Delta}{2}(\hat{b}_{\boldsymbol{k}}^\dagger\hat{b}_{-\boldsymbol{k}}^\dagger + \hat{b}_{\boldsymbol{k}}\hat{b}_{-\boldsymbol{k}}) \tag{2}$$

where the sum extends over momenta in the first Brillouin zone and $\hat{b}_{\boldsymbol{k}} = (1/L)\sum_{\boldsymbol{i}} e^{-i\boldsymbol{k}\cdot\boldsymbol{i}}\hat{b}_{\boldsymbol{i}}$, for an $L \times L$ lattice with dispersion $\varepsilon_{\boldsymbol{k}} = -2J(\cos k_x + \cos k_y)$. Equation (2) shows that each pair of $\pm\boldsymbol{k}$ modes with opposite momentum evolves independently with a Hamiltonian reminiscent to that of a detuned parametric amplifier [31,32]. The corresponding physics is easily understood by analyzing the amplitudes $\psi_{\boldsymbol{k}} = \langle\hat{b}_{\boldsymbol{k}}\rangle$, with equations of motion

$$i\frac{d}{dt}\begin{pmatrix}\psi_{\boldsymbol{k}}\\ \psi_{-\boldsymbol{k}}^*\end{pmatrix} = \begin{pmatrix}\varepsilon_{\boldsymbol{k}} - \nu & \Delta\\ -\Delta & \nu - \varepsilon_{\boldsymbol{k}}\end{pmatrix}\begin{pmatrix}\psi_{\boldsymbol{k}}\\ \psi_{-\boldsymbol{k}}^*\end{pmatrix}. \tag{3}$$

Their general solution can be written as $\psi_{\boldsymbol{k}}(t) = e^{i\lambda_{\boldsymbol{k}}t}u_{\boldsymbol{k}} + e^{-i\lambda_{\boldsymbol{k}}t}v_{\boldsymbol{k}}$, where $u_{\boldsymbol{k}}$ and $v_{\boldsymbol{k}}$ are time-independent coefficients determined by the initial conditions and $\lambda_{\boldsymbol{k}}^2 = (\varepsilon_{\boldsymbol{k}} - \nu)^2 - \Delta^2$. Those $\boldsymbol{k}$ modes satisfying $|\varepsilon_{\boldsymbol{k}} - \nu| \geq \Delta$ evolve in a stable fashion. In contrast, the modes with $|\varepsilon_{\boldsymbol{k}} - \nu| < \Delta$ are dynamically unstable and diverge exponentially with time. The divergence rate $\text{Im}\{\lambda_{\boldsymbol{k}}\}$ is maximized for the $\boldsymbol{k}$ modes satisfying $\varepsilon_{\boldsymbol{k}} - \nu = 0$, which for fermionic models corresponds to the Fermi surface, which we thus dub "Bose surface" here.

The instability at $U = 0$ indicates that the density of bosons will increase indefinitely. In a real system, however, dissipation and nonlinear effects (interactions) make the density saturate, eventually halting the system into a steady state. In particular, the pair driving that we consider here will be accompanied by a two-boson (nonlinear) loss in real implementations, as we highlight in [30]. Mathematically, this has to be treated through a master equation for the mixed state of the system. However, under the assumption that superfluid order is present, we can simplify the problem by invoking the mean-field or coherent-state approximation. As detailed in [30], on the one hand this is equivalent to adding an imaginary part to the interaction, that is, $U = g - i\gamma$ with g and γ real and positive, which makes the Hamiltonian Eq. (1) non-Hermitian, becoming then an effective description of the open system. On the other hand, the coherent-state approximation amounts to replacing the bosonic operators by their expectation value $\psi_{\boldsymbol{i}} = \langle\hat{b}_{\boldsymbol{i}}\rangle$ in the Heisenberg equations. Since our model is defined on a lattice, this leads to a finite-differences version of the Gross-Pitaevskii (GP) equation:

$$i\frac{d\psi_i}{dt} = -J\sum_j\psi_j - \nu\psi_i + (g - i\gamma)|\psi_i|^2\psi_i + \Delta\psi_i^*, \tag{4}$$

where the summation is restricted to the site $\boldsymbol{j}$ adjacent to site $\boldsymbol{i}$. More often than not, driving and dissipation inevitably heat up the system and are thus detrimental to superfluid order. However, focusing on the thermodynamic limit with infinite boson numbers (where dissipative tunneling between symmetry-breaking states takes an infinite time [33–35]) and a regime where the driving, dissipation, and interaction rates are much smaller than the hopping rate (Δ, g, $\gamma \ll J$), superfluidity is expected to survive in the nonequilibrium steady state. Indeed, this is supported by experimental observations in exciton-polariton BECs [14,15,36] and theoretical analysis based on complex GP equations [37,38].

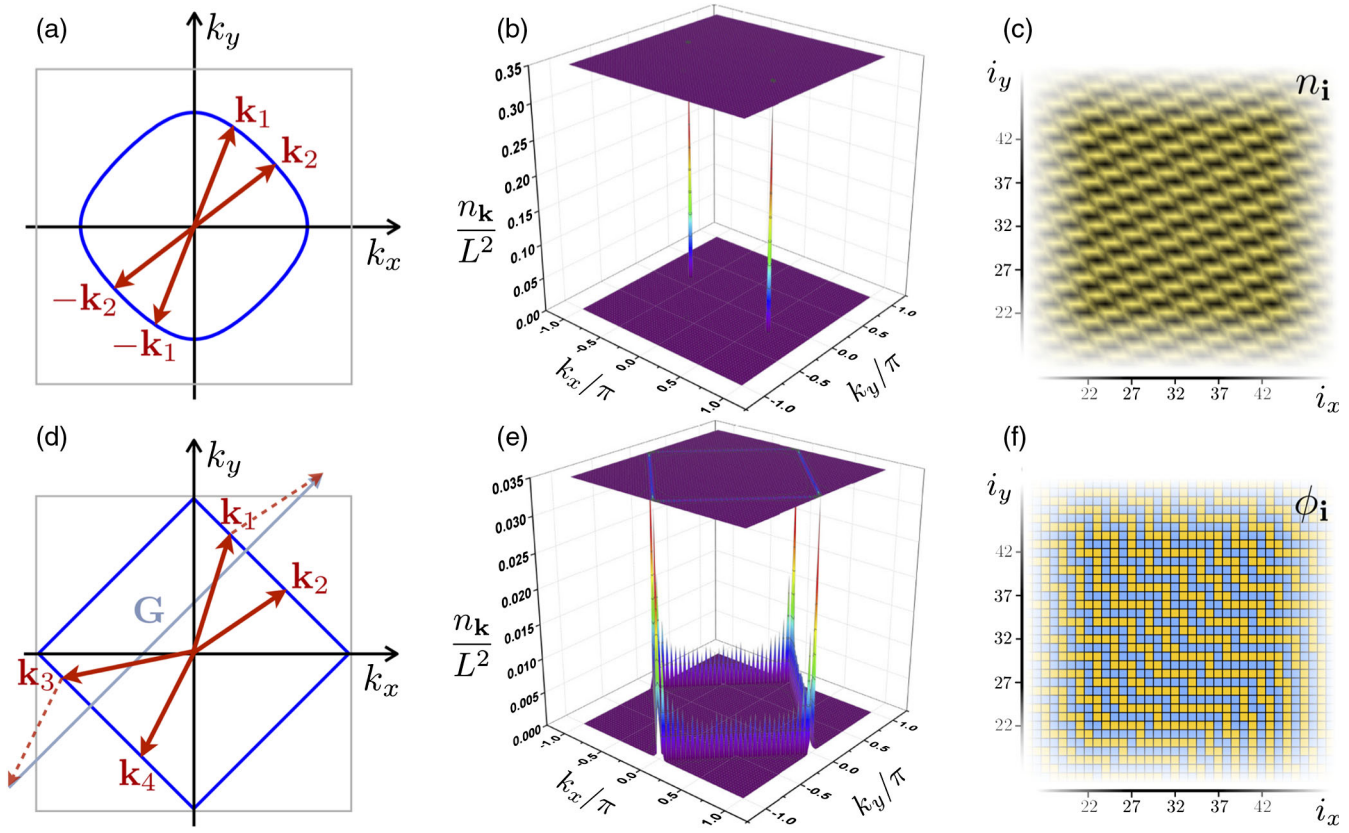

FIG. 1. Two characteristic Bose surfaces (blue solid line, determined by $\varepsilon_k - \nu = 0$) with (a) generic geometry with $\nu \neq 0$ and (d) nested geometry with $\nu = 0$, whose opposite contours are connected by a $\boldsymbol{G}/2 = (\pi, \pi)$ vector. In (b) and (c) we show the steady-state density distribution in momentum and real space (lighter colors correspond to larger densities), respectively, for a generic geometry with $\nu = -J$. We consider the nested-surface case in (e) and (f) where we plot, respectively, the steady-state density distribution in momentum space and the phase distribution in real space, blue (orange) tiles corresponding to a $3\pi/4$ ($-\pi/4$) phase. The parameters are chosen as $\Delta = \gamma = 0.1J$, $g = 0$, and, $L = 64$ (note that real-space plots zoom into the central area of the simulated domain, for which we chose periodic boundaries).

Note as well that for weakly interacting bosonic models, it is known that lattice effect is not important for ground states, which are usually superfluid states with bosons condensed at zero momentum irrespective of the lattice geometry. In contrast, we show below that the lattice effect plays an important role in our nonequilibrium steady state, particularly through the Bose-surface nesting effect, which is absent in a continuous space or nonbipartite lattice (e.g., triangle lattice).

In order to determine the steady-state configuration of the system, we have numerically evolved Eq. (4) until it settles into some final state that we denote by $\lim_{t\to\infty} \psi_i(t) \equiv \bar{\psi}_i$. We have exhaustively analyzed different random initial conditions, especially initial configurations randomly distributed around a uniform complex background ψ_0, that is, $\psi_i(0) = \psi_0 + \delta\psi_i$, with $\delta\psi_i$ having random phases and magnitudes uniformly distributed in the interval $[0, 0.1|\psi_0|]$. For the parameters of interest, we have found that the steady-state properties are independent of the initial state. Of course, patterns spontaneously break the system's translational invariance and can therefore emerge in any of several equivalent configurations (e.g., the orientation of the stripes) randomly selected by the initial fluctuations.

Note that, in momentum space, the nonlinear terms induce scattering between different $\boldsymbol{k}$ modes, leading to a nonlinear competition that is won by modes located at the Bose surface, where the divergence rates are maximized. The geometry of such Bose surface plays then a crucial role in determining the spatial pattern into which the bosons condense. In the following, we study two different Bose surfaces, depicted in Fig. 1(a) and (d). We focus the numerics on moderate values of the interactions ($g < \gamma$, in particular) since otherwise the term $g|\psi_i|^2$ might induce a shift of the chemical potential and bring us off the Bose-surface geometry in which we are interested. This regime is also aligned with realistic experimental conditions [39–41] in the implementation we propose below.

Generic Bose surface versus Bose-surface nesting.— We first consider the $\nu \neq 0$ case, for which the Bose surface forms a closed ring with C_4 rotational symmetry [see Fig. 1(a)]. Since the divergence rates of all the modes at the

Bose surface are identical, one might expect them to have a uniform density distribution. This is additionally supported by the fact that momentum conservation allows now for the so-called "BCS" scattering channel [42] $(\boldsymbol{k}_1, -\boldsymbol{k}_1) \to (\boldsymbol{k}_2, -\boldsymbol{k}_2)$ that couples arbitrary momenta $\pm\boldsymbol{k}_1$ and $\pm\boldsymbol{k}_2$ on the Bose surface.

This intuition is challenged, however, by our numerical results. We show in Fig. 1(b) the steady-state density $n_{\boldsymbol{k}} = |\bar{\psi}_{\boldsymbol{k}}|^2$. In contrast to the expected uniform distribution on the Bose surface, a pair of $\pm\boldsymbol{k}$ modes is spontaneously selected by the random initial conditions as evidenced by the sharp peaks on the plot. In Fig. 1(c), we show the corresponding real-space density $n_{\boldsymbol{i}} = |\bar{\psi}_{\boldsymbol{i}}|^2$, which shows the corresponding striped pattern. In addition to the exhaustive numerical analysis, we have been able to prove analytically [30] that these striped patterns are stable against perturbations with momenta at the Bose surface and also against small-momentum excursions (see below). In contrast, we prove in [30] that even though the expected uniform solution exists, it is unstable. Moreover, in [30] we show that the selected amplitudes have the fixed-phase relation $\bar{\psi}_{\boldsymbol{k}} = -i\bar{\psi}^*_{-\boldsymbol{k}} e^{-i\varphi} = e^{i\phi}\sqrt{\rho/3}$, where $\varphi = \arg\{\gamma + ig\}$ and $\rho = L^2\Delta/\sqrt{\gamma^2 + g^2}$. ϕ is an arbitrary phase that determines the location of the pattern.

The most interesting situation occurs for the square lattice model with $\nu = 0$, where the Bose surface contours coincide when shifted along a fixed reciprocal lattice vector $\boldsymbol{G}/2 = (\pi, \pi)$ [see Fig. 1(d)]. This effect, dubbed "Fermi surface nesting," is known to play an important role in determining the properties of the Fermi-Hubbard model at half-filling [43]. One of the most important consequences of such an effect is that the number of scattering channels increases dramatically, e.g., given three momenta on the Bose surface, one can always find a fourth one such that $\boldsymbol{k}_1 + \boldsymbol{k}_2 = \boldsymbol{k}_3 + \boldsymbol{k}_4 + \boldsymbol{G}$ (Umklapp scattering) [see Fig. 1(d)]. Such scattering channels are allowed in the lattice system since the total momentum is shifted by a reciprocal lattice vector during the scattering process. In the closed fermionic model, these new channels are responsible for the gap opening and the divergence of the density wave susceptibility at momentum $\boldsymbol{G}/2$ [42]. Here, we show that they can also significantly change the properties of the nonequilibrium steady state of our bosonic model.

The steady-state density distribution $n_{\boldsymbol{k}}$ is plotted in Fig. 2(e), where we see that, in contrast to the previous generic Bose surface where condensation occurs only on two $\pm\boldsymbol{k}$ modes, here all the modes on the Bose surface are occupied. Such a steady state is an unconventional BEC, with bosons condensed on a closed ring instead of discrete points. In turn, the real-space density distribution $n_{\boldsymbol{i}}$ is completely uniform [30], while the phase distribution $\phi_{\boldsymbol{i}} = \arg\{\bar{\psi}_{\boldsymbol{i}}\}$ follows the rule that each lattice site must have two pairs of neighbors differing by a π phase, which creates nontrivial phase portraits [Fig. 1(f)]. We have been able to derive this solution analytically, even proving that it

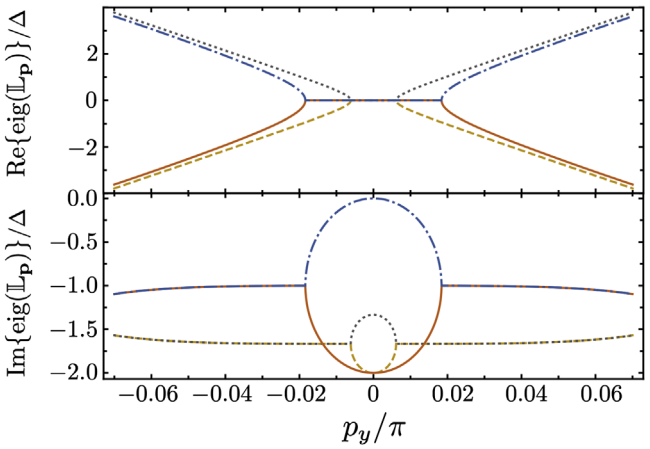

FIG. 2. Real (top) and imaginary (bottom) parts of the relaxation spectrum as a function of momentum excursions p_y (for $p_x = 0$). We consider a square lattice with $\nu = -J$, $\Delta = 0.1$ J, $g = 0$, and $\boldsymbol{k} = (0, 2\pi/3)$. A single imaginary eigenvalue (blue, dashed-dotted line) dominates the spectrum around $\boldsymbol{p} = \boldsymbol{0}$.

is robust against arbitrary perturbations [30]. In equilibrium physics, bosons usually prefer to condense into discrete points to avoid exchange energy. Only when very specific conditions occur (e.g., moatlike band structures with infinitely degenerate minima forming a closed curve) has it been conjectured that the interplay between the degeneracy and quantum correlations leads to a Bose-liquid state of the type we have found here [26,27]. In our nonequilibrium case, such unconventional superfluid states have a completely different origin: a momentum selection mechanism induced by the interplay between nonequilibrium conditions, nonlinear mode couplings, and lattice effects. Energy minimization is no longer a criterion here since the steady state in our model is not related to any ground state.

Given the qualitative difference between the steady states for generic and nested Bose surfaces, one may wonder how they are connected as ν approaches zero. In the parameter regime that we study, $g < \gamma \ll J$, the interaction-induced shift of ν can be neglected, and thus the physics is dominated by its bare value. As a consequence, the transition between these two steady states occurs suddenly at $\nu = 0$ within the mean-field approximation. For different parameter regimes (e.g., the strongly interacting case $g \sim J$), the shift in ν and corrections to the mean-field theory must become relevant, leading to a more complicated transition. Possible scenarios include one in which the discontinuous transition is turned into a crossover with coexistence of both states or one in which the original transition point at $\nu = 0$ is extended into a stable intermediate phase where the $\pm\boldsymbol{k}$ peaks of the striped pattern continuously broaden as ν is reduced toward 0.

Relaxation spectrum.—It is interesting to understand the way in which perturbations relax toward the steady-state condensate. To this aim, and as shown in detail in [30], we

transform Eq. (4) to momentum space and linearize it with respect to fluctuations around a generic Bose surface where bosons have condensed into a pair of modes with opposite momenta $\pm\boldsymbol{k}_0$. Specifically, we expand the amplitudes as

$$\psi_{\boldsymbol{k}}(t) = \bar{\psi}_{\boldsymbol{k}0}\delta_{\boldsymbol{k}_0\boldsymbol{k}} + \bar{\psi}_{-\boldsymbol{k}_0}\delta_{-\boldsymbol{k}_0\boldsymbol{k}} + d_{\boldsymbol{k}}(t) \tag{5}$$

and consider only fluctuations with small-momentum excursions $\boldsymbol{p}$ around $\pm\boldsymbol{k}_0$, that is, $|\boldsymbol{p}| \ll |\boldsymbol{k}_0|$. This leads to a closed linear system $i\dot{\boldsymbol{d}}_{\boldsymbol{p}} = \mathbb{L}_{\boldsymbol{p}}\boldsymbol{d}_{\boldsymbol{p}}$ for the fluctuations $\boldsymbol{d}_{\boldsymbol{p}} = (d_{\boldsymbol{k}_0+\boldsymbol{p}}, d_{-\boldsymbol{k}_0+\boldsymbol{p}}, d^*_{\boldsymbol{k}_0-\boldsymbol{p}}, d^*_{-\boldsymbol{k}_0-\boldsymbol{p}})^T$, with a relaxation matrix $\mathbb{L}_{\boldsymbol{p}}$ that we provide in [30]. The eigenvalues of this matrix determine the relaxation spectrum and are plotted in Fig. 2 for one characteristic example. For all choices of parameters, we find that relaxation is dominated by a single eigenvalue, which can be approximated by a purely imaginary quadratic form: $-i\boldsymbol{p}^T\mathcal{K}\boldsymbol{p}$. The curvature matrix $\mathcal{K}$ depends on the system parameters, but the result is otherwise universal, indicating a purely diffusive, nonpropagating behavior of the elementary excitations of our open system that is similar to what has been shown for exciton-polariton condensates [37,44]. By exhaustive inspection, we have found that the striped patterns are stable (i.e., $\mathcal{K}$ has positive eigenvalues) for $g < \gamma$ but can be destabilized when $g > \gamma$, leading to more complicated patterns that we will study in the future. We have also checked that our results are robust against linear dissipation as long as nonlinear dissipation dominates.

Experimental implementation.—We propose to implement our model with an array of superconducting circuits known as transmons [45] that act as weakly nonlinear quantum oscillators (discussed in more detail in [30]). Pair driving and dissipation are well established for these circuits [39–41], in which the "chemical potential" ν becomes easily tunable through external fields [30]. In addition, current chips allow for 2D lattices with as many as 54 transmons and tunable couplings, as demonstrated in Google's pioneering experiments leading to quantum advantage [46]. This number keeps growing steadily, motivated by the goal of practical quantum computing. Moreover, we remark that transmon arrays have already allowed for proof-of-principle experiments exploring the standard BH model in 1D [47].

We emphasize that our work reveals the intriguing possibility that quantum computation platforms are not only of immense practical significance but also pose their own interest as analog quantum simulators of emergent many-body phenomena far from equilibrium.

Discussion.—We comment now on the relation and differences between our results and other relevant work. Stripe phases, as a consequence of condensation on a pair of modes with opposite momenta, have been observed in both equilibrium [48] and nonequilibrium [22] closed interacting bosonic systems. In both cases, the momenta correspond to the energy minimum of an effective Hamiltonian (e.g., a Floquet Hamiltonian for periodically driven systems [22]). In contrast, in our driven-dissipative model, the pair of momenta is spontaneously selected among extensive degenerate modes at the Bose surface, which is formed by the maximally divergent momenta and thus has nothing to do with the minimum of any Hamiltonian. Hexagonal patterns [14] and solitons [15], which have been observed in continuous-space driven-dissipative exciton-polaritons [36], emerge from the interplay between linear losses, interactions, and a judicious spatiotemporal choice of driving fields. In our system, nonlinear dissipation and the lattice effect are crucial for the stabilization of exotic states with bosons condensed on a closed ring. This state is of great relevance for some open problems in condensed matter and has not been predicted before by any other driven-dissipative mechanism to our knowledge. Currently, lattices can be engineered on exciton-polariton systems [49–51], opening the possibility of implementing our ideas on such platforms as well.

Conclusions and outlook.—In this Letter, we have studied the steady states of a pair-driven-dissipative BH model of relevance for current quantum simulators based on superconducting circuit arrays and leading to unconventional superfluid states of relevance for condensed matter. We have shown that the shape of a so-called "Bose surface" is crucial for the steady-state properties of driven-dissipative bosonic systems, which is similar to the properties of interacting fermions at equilibrium. Future developments will include the analysis of models with flatbands (i.e., bands with constant $\varepsilon_{\boldsymbol{k}}$) in which bosons can potentially condense into spatially localized structures such as solitons.

We thank Germán J. de Valcárcel for useful suggestions. Z. C. is supported in part by the National Key Research and Development Program of China (Grant No. 2016YFA0302001), NSFC of China (Grant Nos. 11674221, No. 11574200), the Project of Thousand Youth Talents, the Program Professor of Special Appointment (Eastern Scholar) at Shanghai Institutions of Higher Learning, and the Shanghai Rising-Star program. We also acknowledge additional support from a Shanghai talent program and the Shanghai Municipal Science and Technology Major Project (Grant No. 2019SHZDZX01).

Z. W. and C. N.-B. contributed equally to this work.

*Corresponding author.
zcai@sjtu.edu.cn

[1] M.Cross and H. Greenside, *Pattern Formation and Dynamics in Nonequilibrium Systems* (Cambridge University Press, Cambridge, 2009).
[2] M. C. Cross and P. C. Hohenberg, Rev. Mod. Phys. **65**, 851 (1993).
[3] J. Swift and P. C. Hohenberg, Phys. Rev. A **15**, 319 (1977).

[4] P. Drazin and W. Reid, *Hydrodynamic Stability* (Cambridge University Press, Cambridge, 2004).

[5] A. Liddle and D. Lyth, *Cosmological Inflation and Large-Scale Structure* (Cambridge University Press, Cambridge, 2000).

[6] A. J. Koch and H. Meinhardt, Rev. Mod. Phys. **66**, 1481 (1994).

[7] K. Staliunas and V. J. Sánchez-Morcillo, *Transverse Patterns in Nonlinear Optical Resonators* (Springer-Verlag, Berlin-Heidelberg, 2003).

[8] P. Mandel, *Theoretical Problem in Cavity Nonlinear Optics* (Cambridge University Press, Cambridge, 1997).

[9] F. Arecchi, S. Boccaletti, and P. Ramazza, Phys. Rep. **318**, 1 (1999).

[10] C. O. Weiss and Y. Larionova, Rep. Prog. Phys. **70**, 255 (2007).

[11] I. Pérez-Arjona, E. Roldán, and G. J. de Valcárcel, Europhys. Lett. **74**, 247 (2006).

[12] I. Pérez-Arjona, E. Roldán, and G. J. de Valcárcel, Phys. Rev. A **75**, 063802 (2007).

[13] C. Navarrete-Benlloch, E. Roldán, and G. J. de Valcárcel, Phys. Rev. Lett. **100**, 203601 (2008).

[14] V. Ardizzone, P. Lewandowski, M. H. Luk, Y. C. Tse, N. H. Kwong, A. Lucke, M. Abbarchi, E. Baudin, E. Galopin, J. Bloch, A. Lemaitre, P. T. Leung, P. Roussignol, R. Binder, J. Tignon, and S. Schumacher, Sci. Rep. **3**, 3016 (2013).

[15] X. Ma, O. A. Egorov, and S. Schumacher, Phys. Rev. Lett. **118**, 157401 (2017).

[16] J. Kronjäger, C. Becker, P. Soltan-Panahi, K. Bongs, and K. Sengstock, Phys. Rev. Lett. **105**, 090402 (2010).

[17] C.-L. Hung, V. Gurarie, and C. Chin, Science **341**, 1213 (2013).

[18] H. Kadau, M. Schmitt, M. Wenzel, C. Wink, T. Maier, I. Ferrier-Barbut, and T. Pfau, Nature (London) **530**, 194 (2016).

[19] J. G. Cosme, C. Georges, A. Hemmerich, and L. Mathey, Phys. Rev. Lett. **121**, 153001 (2018).

[20] Z. Zhang, K.-X. Yao, L. Feng, J. Hu, and C. Chin, Nat. Phys. **16**, 652 (2020).

[21] L. Vidmar, J. P. Ronzheimer, M. Schreiber, S. Braun, S. S. Hodgman, S. Langer, F. Heidrich-Meisner, I. Bloch, and U. Schneider, Phys. Rev. Lett. **115**, 175301 (2015).

[22] L. W. Clark, L. Feng, and C. Chin, Science **354**, 606 (2016).

[23] A. Sheikhan and C. Kollath, Phys. Rev. A **99**, 053611 (2019).

[24] J. Léonard, A. Morales, P. Zupancic, T. Esslinger, and T. Donner, Nature (London) **543**, 87 (2017).

[25] M. P. A. Fisher, P. B. Weichman, G. Grinstein, and D. S. Fisher, Phys. Rev. B **40**, 546 (1989).

[26] T. A. Sedrakyan, L. I. Glazman, and A. Kamenev, Phys. Rev. Lett. **114**, 037203 (2015).

[27] S. Jiang, L. Zou, and W. Ku, Phys. Rev. B **99**, 104507 (2019).

[28] C.-J. Wu, I. Mondragon-Shem, and X.-F. Zhou, Chin. Phys. Lett. **28**, 097102 (2011).

[29] S. Gopalakrishnan, A. Lamacraft, and P. M. Goldbart, Phys. Rev. A **84**, 061604(R) (2011).

[30] See Supplemental Material at http://link.aps.org/supplemental/10.1103/PhysRevLett.125.115301 for further details of the experimental proposal, the corresponding master equation, its connection to the complex Gross-Pitaevskii equation, and the analysis of the various steady-state solutions and their stability.

[31] B. R. Mollow and R. J. Glauber, Phys. Rev. **160**, 1076 (1967).

[32] H. J. Carmichael, G. J. Milburn, and D. F. Walls, J. Phys. A **17**, 469 (1984).

[33] P. Kinsler and P. D. Drummond, Phys. Rev. A **43**, 6194 (1991).

[34] C. Navarrete-Benlloch, T. Weiss, S. Walter, and G. J. de Valcárcel, Phys. Rev. Lett. **119**, 133601 (2017).

[35] F. Iemini, A. Russomanno, J. Keeling, M. Schirò, M. Dalmonte, and R. Fazio, Phys. Rev. Lett. **121**, 035301 (2018).

[36] I. Carusotto and C. Ciuti, Rev. Mod. Phys. **85**, 299 (2013).

[37] M. Wouters and I. Carusotto, Phys. Rev. Lett. **99**, 140402 (2007).

[38] U. C. Täuber and S. Diehl, Phys. Rev. X **4**, 021010 (2014).

[39] Z. Leghtas, S. Touzard, I. M. Pop, A. Kou, B. Vlastakis, A. Petrenko, K. M. Sliwa, A. Narla, S. Shankar, M. J. Hatridge, M. Reagor, L. Frunzio, R. J. Schoelkopf, M. Mirrahimi, and M. H. Devoret, Science **347**, 853 (2015).

[40] R. Lescanne, M. Villiers, T. Peronnin, A. Sarlette, M. Delbecq, B. Huard, T. Kontos, M. Mirrahimi, and Z. Leghtas, Nat. Phys. **16**, 509 (2020).

[41] C. S. Wang, J. C. Curtis, B. J. Lester, Y. Zhang, Y. Y. Gao, J. Freeze, V. S. Batista, P. H. Vaccaro, I. L. Chuang, L. Frunzio, L. Jiang, S. M. Girvin, and R. J. Schoelkopf, Phys. Rev. X **10**, 021060 (2020).

[42] R. Shankar, Rev. Mod. Phys. **66**, 129 (1994).

[43] J. E. Hirsch, Phys. Rev. B **31**, 4403 (1985).

[44] M. H. Szymańska, J. Keeling, and P. B. Littlewood, Phys. Rev. Lett. **96**, 230602 (2006).

[45] P. Krantz, M. Kjaergaard, F. Yan, T. P. Orlando, S. Gustavsson, and W. D. Oliver, Appl. Phys. Rev. **6**, 021318 (2019).

[46] F. Arute *et al.*, Nature (London) **574**, 505 (2019).

[47] R. Ma, B. Saxberg, C. Owens, N. Leung, Y. Lu, J. Simon, and D. I. Schuster, Nature (London) **566**, 51 (2019).

[48] Y.-J. Lin, K. Jiménez-García, and I. B. Spielman, Nature (London) **471**, 83 (2011).

[49] N. Y. Kim, K. Kusudo, C. Wu, N. Masumoto, A. Loffler, S. Hofling, N. Kumada, L. Worschech, A. Forchel, and Y. Yamamoto, Nat. Phys. **7**, 681 (2011).

[50] T. Jacqmin, I. Carusotto, I. Sagnes, M. Abbarchi, D. D. Solnyshkov, G. Malpuech, E. Galopin, A. Lemaître, J. Bloch, and A. Amo, Phys. Rev. Lett. **112**, 116402 (2014).

[51] P. St-Jean, A. Dauphin, P. Massignan, B. Real, O. O. Jamadi, M. Milicevic, A. Lemaître, A. Harouri, L. Le Gratiet, I. Sagnes, S. Ravets, J. Bloch, and A. Amo, arXiv:2002.09528.